Symmetry breaking of the flow in a cylinder driven by a rotating end wall

H. M. Blackburn[a)]
CSIRO Building Construction & Engineering, P.O. Box 56 Highett, Victoria 3190, Australia

J. M. Lopez[b)]
Department of Mathematics, Arizona State University, Tempe, Arizona 85287-1804

(Received 15 May 2000; accepted 26 July 2000)

The flow driven by a rotating end wall in a cylindrical container with aspect ratio $H/R=2.5$ is time dependent for Reynolds numbers $\mathrm{Re}=\Omega R^2/\nu>2700$. For Reynolds numbers up to 4000 three solution branches have been identified, and we examine a solution on each one. At $\mathrm{Re}=3000$, the flow is axisymmetric and time periodic. At $\mathrm{Re}=3500$, the flow is quasiperiodic with a low-frequency modulation and supports a modulated rotating wave with azimuthal wave number $k=5$. At $\mathrm{Re}=4000$, the flow is time periodic with a qualitatively different mode of oscillation to that at $\mathrm{Re}=3500$. It also supports a modulated rotating wave, with $k=6$. The peak kinetic energy of the nonaxisymmetric modes is associated with the jet-like azimuthal flow in the interior.
 [S1070-6631(00)00311-1]

Flow in a cylinder driven by steady end wall rotation has attracted attention since Vogel[1] identified a steady axisymmetric breakdown of the central vortex. Since then, the flow configuration has been regarded as particularly suited to detailed study of vortex breakdown phenomena, in part because the flow is completely enclosed and the boundary conditions well defined. The two dimensionless groups that characterize the problem are the aspect ratio H/R and the Reynolds number $\mathrm{Re}=\Omega R^2/\nu$, where H and R are respectively the height and radius of the cylinder, Ω is the angular speed of one end wall, and ν the kinematic viscosity of the fluid.

The experiments of Escudier[2] demonstrated that if the flow reaches a steady state, it is axisymmetric. Subsequent investigations have mapped out the flow topology of the steady axisymmetric states,[2–4] and examined the onset of unsteady flow when the governing equations are restricted to an axisymmetric subspace.[5–8]

A study of the stability of the steady axisymmetric flow to general three-dimensional time-dependent perturbations has been carried out by Gelfgat.[9] For cylinder aspect ratios near $H/R=2.5$, the onset of time dependence was found to occur via a supercritical Hopf bifurcation near $\mathrm{Re}=2700$, with the axisymmetric mode being the most unstable. To date, the stability of the subsequent time-periodic state has not been studied theoretically.

A recent experimental study[10] of flow in a cylinder with $H/R=2.5$ identified three solution branches in the Reynolds number range 2700–4000. By studying the temporal behavior of dye sheets near the axis of the cylinder, it was discovered that each solution branch has a distinct dominant frequency. The first branch, with $\tau_1=\Omega T_1\approx 36$, has axisymmetric periodic flows from the onset of unsteadiness at $\mathrm{Re}\approx 2700$, and extends to $\mathrm{Re}\approx 3500$. The second branch, with $\tau_2=\Omega T_2\approx 28$, $\mathrm{Re}>3500$, also has periodic flows, but these appeared to be nonaxisymmetric. A third branch, overlapping the other two for $3200<\mathrm{Re}<3700$, has quasiperiodic flows that also appear to be nonaxisymmetric, with fundamental period $\tau_3=\Omega T_3\approx 57$. Three solution branches were also obtained in a set of associated axisymmetric numerical simulations,[10] and it was found that the fundamental periods of oscillation were very close to the experimental observations.

It is not easy to conclusively determine if these flows remain axisymmetric through laboratory experiments. Any small unsteady perturbation, even if axisymmetric, coupled with slightly nonaxisymmetric release of dye or other flow visualization tracer, can produce a readily observed lack of axisymmetry in streaklines or particle paths.[10–12] The experimental method employed in Ref. 10 only delivers information about the temporal behavior of the axisymmetric component of flow, even if the flow is nonaxisymmetric, provided the flow approaches axisymmetry in the near-axis region.

Previous results leave open significant questions concerning the loss of axisymmetry in this flow, and there are a number of recent experimental and numerical results in this and related flows that offer differing views about the symmetry breaking.[13–15] Here we address the issue for geometries with $H/R=2.5$ via direct numerical simulation of the unsteady three-dimensional Navier–Stokes equations.

In the cylindrical geometry, the equations and boundary conditions are invariant to arbitrary azimuthal rotations; in a numerical study of symmetry breaking the equivalent discrete system of equations should preserve the invariance. The most natural and efficient way to ensure this property is to employ a Fourier basis in the azimuthal coordinate. In our numerical method, the velocity $\boldsymbol{u}(z,r,\theta)$ is projected by Fourier transformation in the azimuth onto a set of two-dimensional complex modes $\hat{\boldsymbol{u}}_k(z,r)$. The radial and azimuthal velocity components are combined into two new variables in such a way as to regularize the cylindrical

a)Electronic mail: hugh.blackburn@dbce.csiro.au
b)Electronic mail: lopez@math.la.asu.edu

Navier–Stokes equations at the origin, and to decouple the viscous terms in the corresponding evolution equations.[16]

This Fourier basis in the azimuth is coupled with a spectral element discretization in the meridional plane.[17] Time integration is carried out with a second-order semi-implicit scheme. Nonlinear terms are computed in skew-symmetric form, but not explicitly dealiased in the azimuthal direction in the multiprocessor version of the code used for most of the computations. The computational domain in (r,z) was discretized into 60 spectral elements with Gauss–Lobatto–Legendre interpolants, typically of order 7. Most of the computations used 64 planes of data in the azimuthal direction (resolving modes up to azimuthal wave number $k=32$) and some cases were recomputed with 80 and 128 planes to check the effects of aliasing and influence of higher harmonics. Dealiased calculations were also used to check the effects of aliasing, which was always found to be insignificant for the most energetic modes.

Evolution of the solution was monitored through time series of energies in each Fourier mode k,

$$E_k=\frac{1}{2A}\rho\int_A \hat{\boldsymbol{u}}_k\cdot\hat{\boldsymbol{u}}_k^* r\,dA,$$

where A is the area of the two-dimensional meridional semiplane, ρ is fluid density, r is distance from the axis, and $\hat{\boldsymbol{u}}_k^*$ denotes the complex conjugate of the velocity data in the kth Fourier mode. Energy of the axisymmetric component of the flow is represented by E_0.

Starting from initial conditions that were a rest state to which was added a random perturbation of order 10^{-8} in the $k=1$ mode, we have obtained outcomes on each of the three solutions branches observed in experiments.[10] Here we detail one solution on each branch and leave a more complete exploration of the dynamics on these branches for a more extensive report.

As the flow spun up at Re=3000, perturbations in all nonaxisymmetric modes decayed until their energies, E_k, reached machine-zero level by $\Omega t\approx 4800$, resulting in a time-periodic and axisymmetric flow. The Re=3500 and Re=4000 cases remained nearly axisymmetric until the flow in the whole cylinder had spun up at $\Omega t\approx 600$. After that time the $k=5$ (Re=3500) or $k=6$ (Re=4000) mode began to grow exponentially, and remained the dominant mode after saturation. The elapsed time to saturation was $\Omega t\approx 15\,000$ at Re=3500, and much less, $\Omega t\approx 3200$, at Re=4000. Following saturation, the Re=3500 case further evolved ($\Omega t>20\,000$) to a state with a very low frequency modulation, while the Re=4000 case remained periodic. For brevity, we will present results only from the asymptotic states.

Figure 1 shows time series of energy in the axisymmetric mode E_0 for the three Reynolds numbers, and, for Re=3500 and 4000, the leading three-dimensional mode in the asymptotic states. The length of the time series encompasses two cycles of the long-period modulation for the Re=3500 case, where $\Omega T\approx 1325$. An interesting feature of the time series for the nonaxisymmetric cases is the strong coupling evident between the energy in the axisymmetric and nonaxisymmetric components of the flow. For the Re=3500 case this also extends to the long-period modulation, where there is an oscillatory exchange of energies between the $k=0$ and $k=5$ modes.

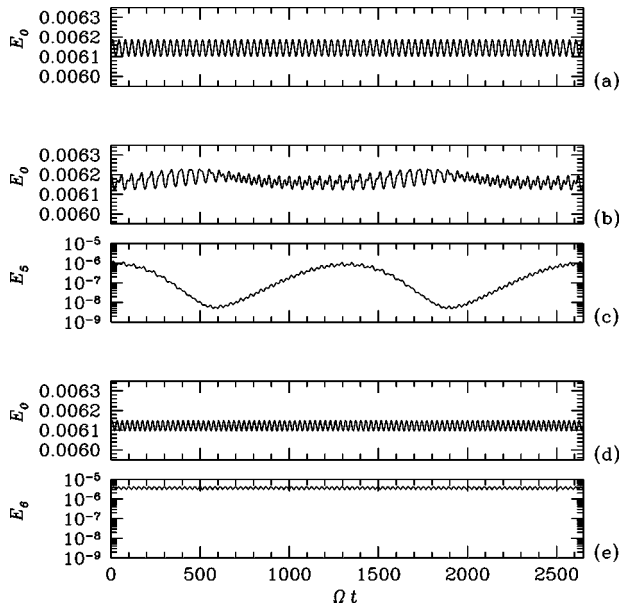

FIG. 1. Time series of the modal kinetic energies for the axisymmetric mode (E_0) and, as appropriate, for the leading nonaxisymmetric mode at (a) Re=3000; (b), (c) Re=3500; (d), (e) Re=4000.

In order to facilitate comparison with previous experimental results we present in Fig. 2 the frequency spectra of the axisymmetric modal energies; as pointed out previously, the experimental technique employed in Ref. 10 provides frequency information about the axisymmetric component of the flow. The fundamental period for each case is: Re=3000, $\Omega T=36.1$; Re=3500, $\Omega T=56.8$; Re=4000, $\Omega T=28.5$. These are in excellent agreement with the measured values presented in Ref. 10, clearly identifying the respective numerical solutions as members of the τ_1, τ_3, and τ_2 solu-

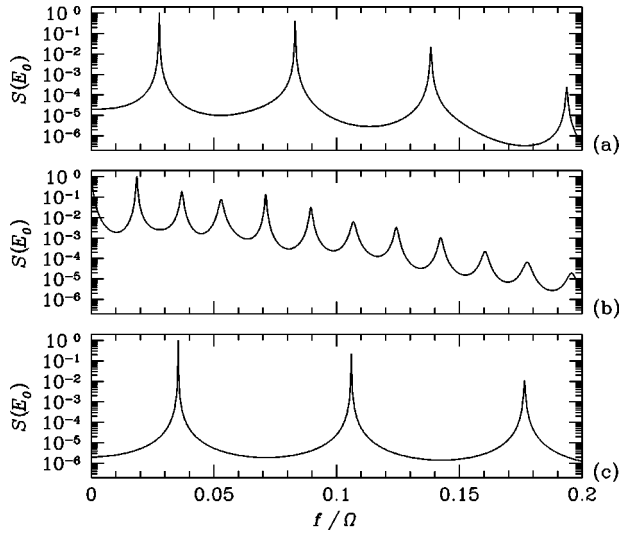

FIG. 2. Spectral density of E_0 time series for (a) Re=3000; (b) Re=3500, and (c) Re=4000.

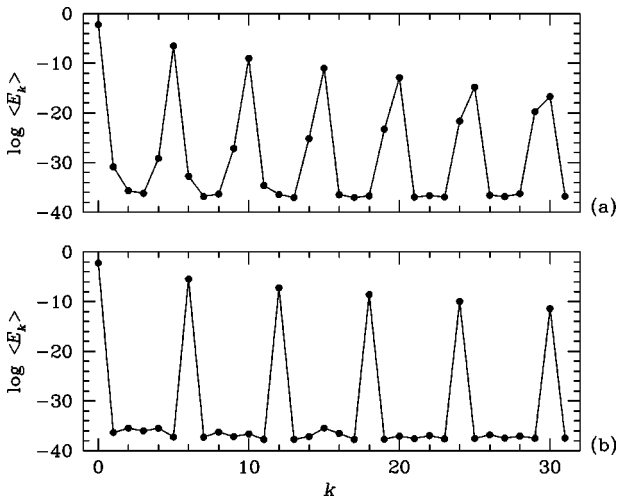

FIG. 3. Azimuthal energy spectra for (a) Re=3500 and (b) Re=4000. The plot for Re=3500 shows some evidence of azimuthal aliasing, while that for Re=4000 is from a dealiased calculation.

tion branches described there. The long-period ($\Omega T = 1325$) modulation for Re=3500 results in the peak near the frequency origin in Fig. 2(b).

Regarding the spatial structure of the nonaxisymmetric solutions, the azimuthal three-dimensionality of the flow can be represented by $5n$ harmonics in the τ_3 case, and $6n$ harmonics in the τ_2 case, as all other modes decay to zero, bar

FIG. 4. Rotating modulated waves of the (a) Re=3500 and (b) Re=4000 solutions, as manifest in the azimuthal velocity component. Above, instantaneous isosurfaces; below, instantaneous contours at elevation $z/H=0.8$. Grid outlines illustrate the extent of the cylinder and spectral element boundaries; the bottom wall rotates clockwise when viewed from above.

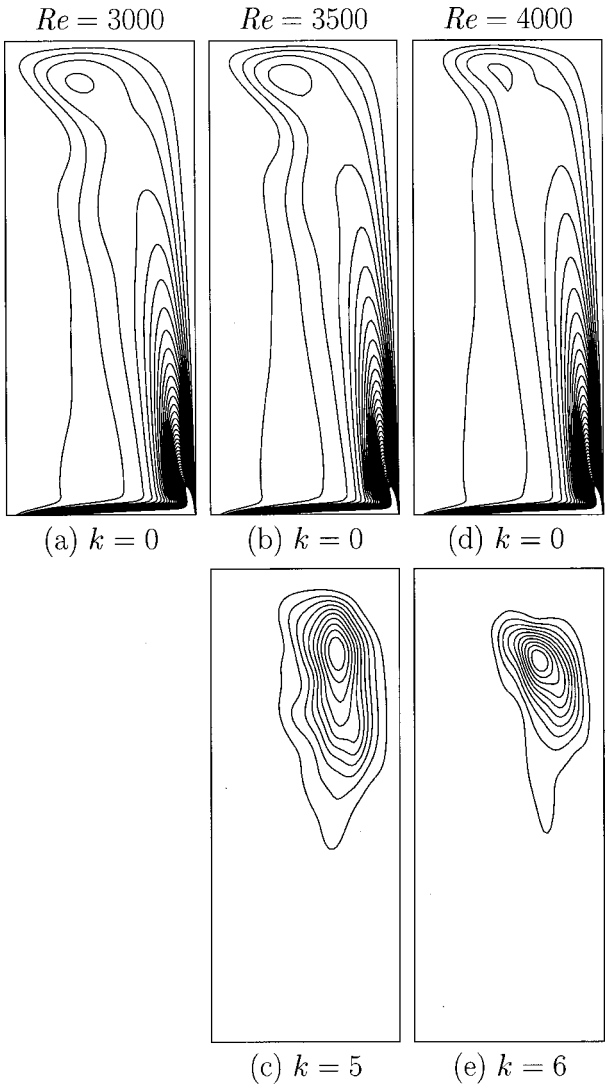

FIG. 5. Contours of averaged flow kinetic energy $\langle 0.5\rho\hat{\mathbf{u}}_k\cdot\hat{\mathbf{u}}_k^*\rangle$ in the meridional semiplane for (a) Re=3000; (b), (c) Re=3500; (d), (e) Re=4000. Upper panel, axisymmetric component; lower panel, energy in the leading nonaxisymmetric mode. In each plot the cylinder axis is to the left and the rotating end wall is at the bottom.

aliasing. Figure 3 illustrates the associated azimuthal energy spectra.

Figure 4 shows isosurfaces and contours of the azimuthal velocity for the τ_3 and τ_2 solutions, which further serve to illustrate the spatial structure of the azimuthal wave in each case. It is apparent that the departure from axisymmetry is greatest in the region near the top stationary end wall. The contours at $z=0.8H$ show that the azimuthal waves are concentrated in the region where the mean azimuthal velocity is a maximum, $r/R\approx 0.67$, and that the region nearest the axis remains nearly axisymmetric.

Figure 5 is a contour plot of the time-averaged kinetic energy in mode $k=0$ for Re=3000, 3500, and 4000, and in modes 5 and 6 for Re=3500 and 4000, respectively. The kinetic energy of mode 0 varies only slightly between the various solutions, the main result to be noted here is that the kinetic energy of the modes 5 and 6 is concentrated near the tip of an azimuthal wall jet that originates from the corner

where the rotating bottom meets the stationary sidewall, as is clearly identified from the mode 0 contours.

The results presented to this point provide no information about azimuthal motion of the rotating waves. The time-dependent states for Re=3500 and Re=4000 described previously have a further frequency associated with the precession of the nonaxisymmetric structure. In both cases the wave precesses in the same direction as the mean azimuthal velocity, and the observed periods are $\Omega T \approx 47.6$ at Re=3500 and 46.4 at Re=4000. These are very close to the period indicated by the mean azimuthal velocity at the location of the peak in the three-dimensional energy, which gives $\Omega T = 44.2$ in both cases. This observation further suggests that the nonaxisymmetric modes are slaved to the underlying axisymmetric state.

Our results suggest that the symmetry breakings on branches τ_2 and τ_3 occur via Naimark–Sacker bifurcations —Hopf bifurcations from a time-periodic base state in which the frequency of the base state survives the bifurcation, and the new frequency following the bifurcation corresponds to the precession frequency. A rotating wave is expected when SO(2) symmetry, e.g., a rotating axisymmetric base state, is broken.[18] However, we have a novel manifestation of this symmetry breaking. Most studied cases involve symmetry breaking from a *steady* axisymmetric state to a rotating wave, which may become modulated following a further Hopf bifurcation, while here symmetry breaking is observed from the *time-dependent* axisymmetric state, leading immediately to modulated rotating waves. To our knowledge, this case has not yet been studied theoretically. The present flow configuration is an ideal canonical case, as the only symmetry it possesses is SO(2) and the dynamics are completely governed by just two control parameters: H/R for the geometry and Re for the driving force.

ACKNOWLEDGMENTS

This work was supported by NSF Grant Nos. DMS-9706951 and CTS-9908599.

[1] H. U. Vogel, ''Experimentelle ergebnisse über die laminare Strömung in eine zylindrischen Gehäuse mit darin rotierender Scheibe,'' Technical Report No. 6, Max-Planck-Inst., 1968.
[2] M. P. Escudier, ''Observations of the flow produced in a cylindrical container by a rotating end wall,'' Exp. Fluids **2**, 189 (1984).
[3] H. Lugt and M. Abboud, ''Axisymmetric vortex breakdown with and without temperature effects in a container with a rotating lid,'' J. Fluid Mech. **179**, 179 (1987).
[4] J. M. Lopez, ''Axisymmetric vortex breakdown: 1. Confined swirling flow,'' J. Fluid Mech. **221**, 533 (1990).
[5] J. M. Lopez and A. D. Perry, ''Axisymmetric vortex breakdown. 3. Onset of periodic flow and chaotic advection,'' J. Fluid Mech. **234**, 449 (1992).
[6] N. Tsitverblit, ''Vortex breakdown in a cylindrical container in the light of continuation of a steady solution,'' Fluid Dyn. Res. **11**, 19 (1993).
[7] J. N. Sørensen and E. A. Christensen, ''Direct numerical simulation of rotating fluid flow in a closed cylinder,'' Phys. Fluids **7**, 764 (1995).
[8] A. Y. Gelfgat, P. Z. Bar-Yoseph, and A. Solan, ''Stability of confined swirling flow with and without vortex breakdown,'' J. Fluid Mech. **311**, 1 (1996).
[9] A. Y. Gelfgat (private communication).
[10] J. L. Stevens, J. M. Lopez, and B. J. Cantwell, ''Oscillatory flow states in an enclosed cylinder with a rotating end wall,'' J. Fluid Mech. **389**, 101 (1999).
[11] G. P. Neitzel, ''Streak-line motion during unsteady and unsteady axisymmetric vortex breakdown,'' Phys. Fluids **31**, 958 (1988).
[12] K. Hourigan, L. J. W. Graham, and M. C. Thompson, ''Spiral streaklines in pre-vortex breakdown regions of axisymmetric swirling flows,'' Phys. Fluids **7**, 3126 (1995).
[13] A. Spohn, M. Mory, and E. J. Hopfinger, ''Experiments on vortex breakdown in a confined flow generated by a rotating disk,'' J. Fluid Mech. **370**, 73 (1998).
[14] F. Sotiropoulos and Y. Ventikov, ''Transition from bubble-type vortex breakdown to columnar vortex in a confined swirling flow,'' Int. J. Heat Fluid Flow **19**, 446 (1998).
[15] J. C. F. Pereira and J. M. M. Sousa, ''Confined vortex breakdown generated by a rotating cone,'' J. Fluid Mech. **385**, 287 (1999).
[16] S. A. Orszag, ''Fourier series on spheres,'' Mon. Weather Rev. **102**, 56 (1974).
[17] A. G. Tomboulides, ''Direct and large-eddy simulation of wake flows: Flow past a sphere,'' Ph.D. thesis, Princeton, 1993.
[18] E. Knobloch, ''Bifurcations in rotating systems,'' in *Lectures on Solar and Planetary Dynamos*, edited by M. R. E. Proctor and A. D. Gilbert (Cambridge University Press, Cambridge, 1994), p. 331.